

This article is a preprint. Please cite the published version:<https://doi.org/10.1016/j.epsr.2021.107053>

Multi-year stochastic design of off-grid microgrids subject to significant load growth uncertainty

Davide Fioriti^{a,*}, Davide Poli^a, Pablo Duenas-Martinez^b,
Ignacio Perez-Arriaga^b

^a*DESTEC, University of Pisa, Largo Lucio Lazzarino, 56122 Pisa, Italy*

^b*MIT Energy Initiative, Massachusetts Institute of Technology, 77 Massachusetts Avenue,
02139, Cambridge, MA, United States*

Abstract

The optimal planning of off-grid microgrids in developing countries is particularly challenging, as several political and socio-economic risks can hamper investments of private companies. Estimating the demand of newly electrified communities is one of the most difficult tasks. Principally, the load growth, which can be very steep, is of serious concern. In this paper, we address this specific challenge and propose a novel stochastic dynamic method to size microgrids within a multi-year perspective, where the demand growth forecasting is subject to uncertainty. In detail, a predefined scenario tree structure allows capturing load growth uncertainty and obtaining different capacity expansion strategies for each scenario. An illustrative case study for an isolated system in Kenya using data collected in 23 Kenyan microgrids is shown. The optimal design achieved with the proposed formulation has an initial capacity that is half of the one obtained through the standard single-year methodology, thus reducing the net present cost by 16-20%. This study is therefore of interest to institutions, developers and researchers that seek fostering rural electrification.

Keywords: Generation Expansion, real option analysis, mini-grid, demand growth, rural electrification, Particle Swarm Optimization (PSO)

Nomenclature

δ^T time resolution [h]

η_i efficiency of asset type i [-]

$c^F; c_i^M$ fuel price [\$/l] and specific maintenance cost of asset type i

*Corresponding author

Email addresses: davide.fioriti@ing.unipi.it (Davide Fioriti), pduenas@mit.edu (Pablo Duenas-Martinez)

$c^{LLC}; c^{HLC}$ low and high priority load curtailment charge [\$/kWh]
 $C_i^{base}; X_i^{base}; \beta_i$ parameters of the CAPEX cost function of component type i
 $C_{nc,t}^{F/M/LC}$ costs of fuel, maintenance and load curtailment in branch nc and time t [k\$]
 $CAP_n; OP_n$ capital and operational charges at node n [k\$]
 $ch(n)$ all children nodes of node n
 $d; c; n$ ids of nodes of the tree representing the multi-year behavior of the microgrid
 $E_{B,nc,t}^{dg}$ degraded capacity of battery [kWh]
 $f^{sl}; f^{int}$ parameters of the fuel consumption map [\$/kW]
 $F_{d,nc,t}^G$ fuel consumption in branch nc and time t of the generator installed in node d [l/h]
 i type of component {B: Battery, D: battery converter, G: Genset, I: Inverter, T: Tank, P: PV}
 L_i lifetime of component type i
 $LL_{i,d,nc,t}$ lifetime loss in current time step [h]
 $N_{i,nc,y}^{Rep}$ number of replacements of asset i , year y
 nc branch from node n to children c
 NPC_n^R NPC of subtree beyond node n [k\$]
 $p(n)$ parent node of node n
 $P_{i,d,nc,t}$ power scheduling of resource i [kW]
 $P_{i,nc,t}^{dg+ / dg-}$ maximum and minimum power rating of components [kW]
 $P_{i,nc,t}^{dg}$ degraded capacity of assets [kW]
 $p_{nc,t}^{Av}$ available renewable production (kW/kWp)
 $P_{nc,t}^{LL/HL}$ low and high priority load [kW]
 $P_{nc,t}^{LLC/HLC}$ low and high priority load curtailment in branch nc and time t [kW]
 $pa(n)$ all parent nodes of node n
 $RES_n; REP_{nc,y}$ residual value of assets and replacement costs at year y and node n [k\$]

- $RL_{i,d,nc,t}$ remaining lifetime in current time step [h]
- $t; y$ hour of the simulation, corresponding year
- $X_{i,d,nc,t}^{dg}$ degraded capacity in branch nc and time t of component type i installed in node d
- $X_{i,n}$ capacity of component type i at node n
- $z_{d,nc,t}^G$ unit commitment of generator $\{1, 0\}$
- $z_{L,i,d,nc,t}^L$ operating status of asset i $\{1, 0\}$

1. Introduction

Microgrids are seen as a promising solution for fostering rural electrification in remote areas in developing countries, as they often prevent the construction of expensive grids extensions that would economically supply only some villages [1]. However, electrifying rural communities that have never experienced electricity is very challenging, especially within a typical time horizon beyond 10 to 15 years [2]. In such long period, social habits and productive uses of electricity change, sometimes sharply, with growth rates above 14-15%/y [3], but very uncertain at the same time, as some projects have experienced no growth causing business failures [1]. Furthermore, microgrid investments often rely on capital-intensive assets with low operating costs, such as batteries and solar panels. However, the capital can be jeopardized if the demand remains low, social and political distress arise, or thefts and vandalism reign. For this reason, optimization techniques that consider uncertainties and a multi-year perspective are helpful approaches to reduce total costs and risks for developers.

Considering the uncertain long-term load growth when optimally designing an off-grid microgrid is of critical importance, but challenging and consequently usually disregarded. Although the microgrids usually last for several years, this multi-year behavior is usually approximated with a single one-year hourly scenario of load and renewable production [1, 4, 5]; thus causing loss of accuracy due to an incomplete forecast that has a negative effect on the simulation of the components behavior. Accordingly, the assets degradation both in decreasing capacity and efficiency over time is usually neglected or extremely simplified when modeling, e.g. the expenditures in replacements or retrofits, which affects the infield profitability of the project.

Planning for future upgrades of the system, including uncertainties in the system dynamics and the degradation of components, can allow deferring investment costs and reducing risks, which mitigate both the fiscal burden and the risk profile of microgrid projects. All above reasons, lead to conclude that it is useful and timely to investigate new methodologies on detailed multi-year analysis on microgrids design, as well as to compare them with traditional yearly simulations to recommend guidelines to researchers, institutions and developers.

1.1. Literature analysis

Multi-year network and generation planning in power systems is a long-established topic in developed countries [6–9]. These methodologies calculate both the initial design of the system and the optimal expansion over time, be it of the grid or the generation. As the combined optimization of grid and capacity expansion is computationally demanding, authors usually approximate the multi-year behavior of the system by a number of representative days [8, 10] or using monthly [11, 12] or yearly [13] duration curves.

Recently, the same topic has been addressed from the microgrids perspective: either interconnected to the main grid [14–19] or isolated [10, 20–24]. Yet, similar simplifications has been taken. The study in [21] applies mixed-integer linear programming (MILP) to optimize only the initial storage capacity of an isolated wind-diesel system, subject to load growth uncertainty using a tree-based approach drawn by a scenario-reduction method. However only a single representative day was used for each scenario. Authors in [20] proposed a similar MILP model where only batteries and their optimal year of installation are optimized. Yearly scenarios, represented by 12 days, were used to address uncertainties in load demand, wind and renewable production, although the load growth rate was considered constant. Contrarily to [21], authors in [20] included a simplified model for the battery degradation; however, these results are limited because only a few typical days represent each year. While the above approaches focused on batteries only, reference [22] proposed the optimization and repowering of the entire off-grid system, including wind turbines and diesel generators, again using representative days. The authors in [25] considered a similar system but including also equipment, yet with a simplified time horizon and with no stochastic perspective. In [17], a multistage stochastic planning approach has been proposed still based on few representative days (1-3), to reduce the computational burden. Instead, the authors in [19] proposed a methodology that decomposes the multi-year optimization to a number of single-year optimizations with interesting results; however, the method does not take into account uncertainties and it is still based on representative days. Furthermore, in [23], the so-called Particle Swarm Optimization (PSO) [1], is used for solving a multi-year capacity expansion problem with the limitation that each year is optimized independently. An interesting approach has been proposed in [24] to tackle multi-year sizing of an off-grid system based on a custom iterative approach modeling capacity fading of the storage only and reliability concerns. This approach is however deterministic and does not consider long-term uncertainties in the load demand has not been considered and the approach is deterministic. Furthermore, another stochastic approach is proposed in [18] that accounts for an interconnected microgrid with a solar plant, a wind turbine, a micro-turbine, a battery storage and electric vehicles in which no degradation is considered, one single day is simulated for each year and the upgraded capacity is not tailored for different scenarios.

The usual way of approximating years with representative days allowed authors to reduce the computational burden, at the cost of reducing the accuracy

of the simulations, especially for battery degradation. This is particularly significant for MILP approaches in which the computational burden significantly grows with the problem size, making it difficult to represent both the entire multi-year time-span and components' degradation within a stochastic formulation [26]. According to the study in [27] that compared different methodologies for optimizing the size of a rural microgrid, the formulation using heuristic algorithms obtained nearly the same solution of the MILP-based model, but with a time reduction from 50% to 99% with respect to the latter. Therefore, we regard heuristic methodologies as a viable option for stochastic multi-year optimization that requires nevertheless further investigation.

As above described, the current state of the art only considers degradation effects for the fading capacity of batteries using a simplified linear model proportional to the installation year, and only for representative days [20]. The exception is [24], which does not implement any stochastic approach, does not apply standard heuristic methods, and only provides a limited comparison with standard methodologies. Other complex formulations rely on rainflow algorithms [28]. However, the corresponding problems would be more complex and require long simulations, which increase computational requirements, particularly on a multi-year analysis. As in typical off-grid microgrids, batteries are discharged deeply every day, the maximum throughput model shows in contrast a good compromise between complexity and computational requirements [24, 28]. This model is implemented in this paper. The aging effects on the photovoltaic panels and converters are mainly related to the thermal stress on components, and they can be represented as a linear degradation with time [29, 30].

1.2. Contributions

To the authors' best knowledge, no other paper has proposed a dynamic stochastic planning methodology for off-grid microgrids, including a detailed load growth representation, the dynamic system upgrade, the components degradation, and the renewable uncertainty. The aim of this paper is to provide a new methodology able to jointly reduce costs and risks for developing microgrid projects. The main contributions are summarized below.

1. A scenario-based stochastic model based on PSO, combined with Monte Carlo scenarios, to optimally size both the initial design and the repowerings of a typical off-grid system.
2. Detailed simulation of the actual system operation for the entire multi-year horizon at hourly time resolution.
3. Assets capacity and efficiency degradation.
4. Simulation of assets' replacements occurring when the components age during the real-time operation.
5. Comparison between multi-year approaches (deterministic and stochastic) and the traditional one-year methodologies.

The methodology is illustrated with a case study of a real off-grid system in Kenya.

The rest of the paper is organized as follows. Section II describes the model whose mathematical formulation is detailed in Section III. Then, the case study is described in Section IV and the results are discussed in Section V. Finally, conclusions are drawn.

2. Problem statement

2.1. Description

The proposed approach has been developed for addressing the unique characteristics of microgrids in developing countries in which the load estimation and its growth are very difficult to forecast. We have considered the configuration of a typical microgrid (Fig. 1), composed by a photovoltaic plant, battery storage, fuel-fired generator and tank storage [1]. Although the proposed approach can easily include other renewable energy sources, for the sake of simplicity, we focus on solar as the preferred choice due to its wide availability in developing countries and low maintenance.

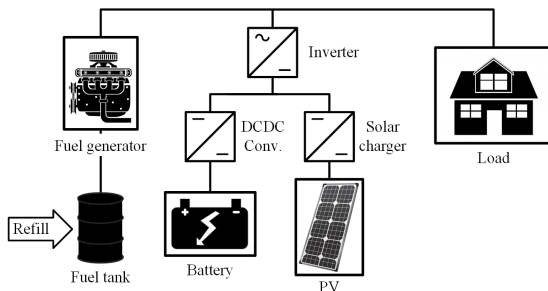


Figure 1: Topology of the microgrid.

As typically done in the literature, the proposed formulation considers active power flows, while the reactive power is assumed to be dispatched by the inverter or the fuel-generator using well-established droop-control techniques [31]. Typical rural loads require limited reactive power and power lines are not long, hence leading to limited consequences in terms of energy flows.

2.2. Load and renewable production tree model

The simulation of the entire stochastic process can lead to unbearable computational requirements. Accordingly, we aim at representing the multi-year behavior of the system by means of scenarios modelled by a tree, similarly to multi-stage optimization [5, 20]. However, conversely to traditional approaches based on representative days, the entire lifetime of the project is simulated at hourly time resolution, hence enabling a detailed representation of the components, load and renewable production. The proposed tree can account for uncertainties in the load growth and the available renewable production with a

structure, as shown in Fig. 2, in which every branch represents a scenario characterized by the occurrence probability and the load scenario. Since we focus on off-grid systems of developing countries in which uncertainties related to the load growth dominate those related to the photovoltaic production, the uncertainties of renewable source are disregarded. However the proposed formulation can easily incorporate additional nodes and branches to account for errors in the renewable production.

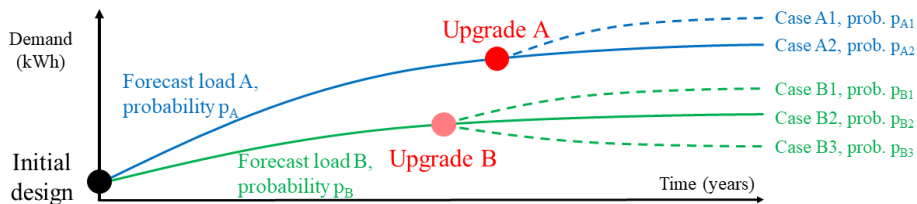


Figure 2: Tree structure of the proposed model: load growth scenarios correspond to branches and repowerings happen at nodes.

Provided a large-enough dataset of data, different scenario reduction techniques can be used to identify the reduced tree with desired characteristics [22, 32], such as the maximum number of leaf nodes and/or branch probabilities, that reduce the computational burden. Considering the limited dataset available for rural microgrids in developing countries and for the sake of clarity, the number of load growth scenarios, as well as the branch probabilities, are preset.

2.3. Objective function

The objective function of the proposed stochastic multi-year problem for a microgrid is the minimization of the expected Net Present Cost (NPC) of the system (1). The NPC considers the initial installation and future upgrades costs $CAPEX_y$, the operational and maintenance cost $OPEX_y$, the replacement charge when components age REP_y , and the residual value of the assets RES_y at the end of the project. It is worth noticing that the term "replacement" refers to when a component previously installed ages and it is replaced with a new component that is identical to the previous one; while "upgrade" refers to a new repowering of the system, with new components, whether or not the previous aged yet. All costs but CAPEX are directly or indirectly affected by the operating strategy as it affects the dispatching and life expectancy and aging of components. The mathematical representation considering the proposed tree structure is detailed in the subsequent section.

$$\min_{\omega \in \Omega} E [NPC] \quad (1)$$

2.4. Microgrid upgrade

In the nodes of the scenario-tree, the algorithm is allowed to upgrade the design of the microgrid. It is worth noticing that the upgraded capacity and year

of installation is independent for each scenario, as observed in Fig. 2, where upgrade B may show different capacity and occur at a different time than upgrade A. In contrast to some previous approaches [21, 22], this allows to dynamically improve the system, considering the actual load growth and reducing risks. For the sake of simplicity, the upgrades can be temporarily preset, e.g. for a specific year. While the simulated investment costs reduce by implementing the number of preset upgrading years, the computational burden increases, too.

2.5. Degradation model

The capacity and efficiency degradation are simulated considering the major aging determinant of each component, which are time for PV panels, converters and diesel tanks, the energy throughput for the battery, and the number of operating hours for the generator [1, 28]. When the aging variable reaches the lifetime value, the corresponding component ages and it cannot be used further unless replacement occurs.

2.6. Replacements

When components age within the simulation phase and before the next system upgrade, the proposed formulation could replace them with a new component identical to the aged unit. Since the last repowering is usually more up-to-date than the previous installation, only the last installed component is replaced, when it ages. Instead, no replacement occurs for components that have already been upgraded. Put simply, let us suppose that a generator was initially installed and it ages in 7 years. If no other generator was installed before the 7th year, the genset is replaced; but if a new generator was installed due to a repowering at the 5th year, the old generator is not upgraded. It is assumed that an adequate procurement of spare parts is performed by the operator.

2.7. Operating strategy

The proposed approach is aimed at simulating the real-time operation of the microgrid and has been designed to accommodate different operating strategies. According to the proposed scenario-tree formulation, the system operation is simulated in the branches.

In our case study, the system is dispatched with the most used operating strategy for rural microgrids: the load-following operating strategy [1, 33], whose aim is to minimize the operating costs with simple priority-list rules. The procedure first dispatches renewable energy sources, then the energy stored in the battery, and finally the generator. For simplification purposes, multiple components of the same type are dispatched proportionally to their actual capacity including degradation; except for generators, which are dispatched independently. More details can be found in [1]. Other approaches, e.g. predictive-based, require significant higher computational requirements that may not justify the slightly higher benefits [1, 33].

3. Mathematical formulation

3.1. Optimzation algorithm

Being accepted and widely used for optimizing complex large problems [1, 9, 34] with very similar results with respect to equivalent MILP approaches [27], Particle Swarm Optimization (PSO) method has been used to calculate the optimal initial design and all capacity expansions of the microgrid. In each PSO iteration, a combination of configurations of the components' initial design and the subsequent repowerings are specified, with the aim of improving the results of the previous iterations. Then, each configuration is simulated for the multi-year horizon as described below. The iterative algorithm stops when the objective function is within a tolerance threshold, e.g. 0.1%, for 20 consecutive iterations. Simulations were performed with hourly time steps.

3.2. Objective function

As shown in (2) and sketched in Fig. 2, the formulation of NPC_n^R recursively calculates the expected NPC of the system for the sub-tree starting in node n . The NPC accounts for the investment costs $CAPEX_n$, the operational and maintenance costs $OPEX_{nc,y}$, the replacements costs $REP_{nc,y}$, the residual value of the assets RES_n and, finally, the same function NPC_n^R evaluated for the sub-tree starting from each children c . The recursive evaluation stops only when the simulation reaches the leaves of the tree ($ch(c) = \emptyset$). Subscript nc denotes the branch that has n and c as parent and child nodes, respectively.

$$\left\{ \begin{array}{l} \min_{\omega \in \Omega} E[NPC] \simeq \min_A [NPC_{n=1}^R] \\ NPC_n^R = CAPEX_n + \sum_{c \in ch(n)} p_{nc} \left[\sum_{y=1}^{N_{i,nc}} \frac{OPEX_{nc,y} + REP_{nc,y}}{(1+d)^y} + \right. \\ \left. \frac{1}{(1+d)^y} \begin{cases} NPC_c^R & ch(c) \neq \emptyset \\ RES_c & ch(c) = \emptyset \end{cases} \right] \end{array} \right. \quad (2)$$

Furthermore, it is worth noticing that all the factors, but CAPEX, are weighted by the occurrence probability p_{nc} of the branch nc . The discount rate d in the objective function penalizes cash flows far in time, while CAPEX has no weight nor discount factor as it refers to the current node n .

The CAPEX formula shown in (3) is assumed invariant with time. $X_{i,n}$ is the capacity of the asset i installed in node n , for a given scenario and year; C_i^{base} is the base cost of the same component with capacity X_i^{base} , and β_i shapes the effect of economies of scale and transportation.

The OPEX detailed in (4) accounts for the fuel costs $C_{nc,t}^F$, the maintenance fees $C_{nc,t}^M$, and the economic value of the energy-not-served $C_{nc,t}^{LC}$. That formulation, whose cost factors are detailed in equations (6) and (7), refers to a

generic branch of the tree spanning from node n to each child c and to every simulation year y of the corresponding scenario. c^F is the fuel price; c^{LLC} and c^{HLC} are the low and high priority load curtailment fees, respectively. c_i^M is the maintenance fee for each component i as a function of the operating status $z_{i,d,nc,t}^L$, which equals zero when the component is not in operation or aged, and one otherwise.

The total expense due to replacements in (8) is a function of the CAPEX of the component i installed in node n and the number of yearly replacements $N_{i,nc,y}^{Rep}$ of the component. The residual value of the assets RES_n is evaluated with (9) at each leaf node n . It is a function of the remaining life $RL_{i,d}$ of each component, the corresponding maximum lifetime L_i of the same type of asset i , a depreciation factor k_i^{Salv} lower than 1, and the investment cost of the component.

$$CAPEX_n = \sum_{i \in A} C_i^{base} \left(\frac{X_{i,n}}{X_i^{base}} \right)^{\beta_i} \quad (3)$$

$$OPEX_{nc,y} = \sum_{t \in T(y)} [C_{nc,t}^F + C_{nc,t}^M + C_{nc,t}^{LC}] \quad (4)$$

$$C_{nc,t}^F = c^F \sum_{d \in pa(c)} F_{d,nc,t}^G \quad (5)$$

$$C_{LC,nc,t} = c^{LLC} P_{nc,t}^{LLC} + c^{HLC} P_{nc,t}^{HLC} \quad (6)$$

$$C_{nc,t}^M = \sum_{d \in pa(c)} \sum_{i \in A} c_i^M X_{i,d} z_{i,d,nc,t}^L \quad (7)$$

$$REP_{nc,y} = \sum_{i \in A} \sum_{d \in pa(c)} N_{i,nc,y}^{Rep} C_i^{base} \left(\frac{X_{i,d}}{X_i^{base}} \right)^{\beta_i} \quad (8)$$

$$RES_n = - \sum_{d \in pa(c)} \sum_{i \in A} k_i^{Salv} \frac{RL_{i,d}}{L_i} C_i^{base} \left(\frac{X_{i,d}}{X_i^{base}} \right)^{\beta_i} \quad (9)$$

3.3. Power balance

The power balance at the AC and DC busbars is guaranteed by equations (10) and (11), respectively. In particular, the scheduling $P_{G,d,nc,t}$ of each generator and the total inverter production $P_{I,nc,t}$ supply the high and low priority load, $P_{nc,t}^{LL}$ and high $P_{nc,t}^{HL}$, respectively. When power or energy restrictions occur, the operating strategy increases first low priority load curtailment $P_{nc,t}^{LLC}$, and secondly the high priority one $P_{nc,t}^{HLC}$. The power balance of the battery $P_{BDC,nc,t}$ at the DC busbar, of the inverter $P_{IDC,nc,t}$ and the photovoltaic

plants $P_{P,d,nc,t}$ installed at the current node is guaranteed by (11).

$$\sum_{d \in pa(c)} P_{G,d,nc,t} + P_{I,nc,t} = \quad (10)$$

$$P_{nc,t}^{LL} + P_{nc,t}^{HL} - P_{nc,t}^{LLC} - P_{nc,t}^{HLC}$$

$$\sum_{d \in pa(c)} P_{P,d,nc,t} + P_{BDC,nc,t} + P_{IDC,nc,t} = 0 \quad (11)$$

3.4. Converters

The total production $P_{I,nc,t}$ of the inverters at AC busbar and of the battery converter at the DC busbar $P_{BDC,nc,t}$ are constrained to be within its actual capacities, as stated in (12) and (14), respectively. The power limits account for the degradation of components as stated in Section 3.9. The batteries dispatch is calculated according to the average actual efficiency $\eta_{B,nc,t}$ of the battery and the DC/DC converter using (15). The model also accounts for the inverter losses in (13).

$$-P_{I,nc,t}^{dg-} \leq P_{I,nc,t} \leq P_{I,nc,t}^{dg+} \quad (12)$$

$$P_{IDC,nc,t} = \begin{cases} \frac{P_{I,nc,t}}{\eta_{I,nc,t}} & P_{I,nc,t} \geq 0 \\ P_{I,nc,t} \eta_{I,nc,t} & P_{I,nc,t} < 0 \end{cases} \quad (13)$$

$$-P_{BDC,nc,t}^{dg-} \leq P_{BDC,nc,t} \leq P_{BDC,nc,t}^{dg+} \quad (14)$$

$$P_{B,nc,t} = \begin{cases} \frac{P_{BDC,nc,t}}{\eta_{B,nc,t}} & P_{BDC,nc,t} \geq 0 \\ P_{BDC,nc,t} \eta_{B,nc,t} & P_{BDC,nc,t} < 0 \end{cases} \quad (15)$$

3.5. Battery

The energy available in the battery $E_{B,nc,t}$ is detailed in (16) as the sum of the four elements: the energy available in the battery in the previous time step $E_{B,nc,t}^{pre}$, be it in the current branch or the previous one, the power flow $P_{B,nc,t}$ of the DC/DC converter deprived by conversion losses, and the additional energy $E_{B,nc,t}^{rep}$ introduced by newly installed batteries due to an upgrade or a replacement. Moreover, the current energy capacities of the battery are guaranteed in (17) according to the degradation model in Section 3.9.

$$E_{B,nc,t} = E_{B,nc,t}^{pre} - P_{B,nc,t} + E_{B,nc,t}^{rep} \quad (16)$$

$$E_{B,nc,t}^{dg-} \leq E_{B,nc,t} \leq E_{B,nc,t}^{dg+} \quad (17)$$

3.6. Renewable production and load curtailment

The hourly renewable production $P_{P,d,nc,t}$ is limited by the maximum hourly available production, which depends on the current capacity of the PV modules $P_{P,d,nc,t}^{dg}$ and the per unit production $p_{nc,t}^{Av}$ referred to a 1-kWp non-degraded module, as shown in (18). The degradation model of $P_{P,d,nc,t}^{dg}$ is detailed in

Section 3.9. The high and low priority load curtailment, $P_{nc,t}^{LLC}$ and $P_{nc,t}^{HLC}$ respectively, are limited by the maximum corresponding load, as detailed in (19) and (20).

$$0 \leq P_{P,d,nc,t} \leq p_{nc,t}^{Av} \sum_{d \in pa(c)} P_{P,d,nc,t}^{dg} \quad (18)$$

$$0 \leq P_{nc,t}^{LLC} \leq P_{nc,t}^{LL} \quad (19)$$

$$0 \leq P_{nc,t}^{HLC} \leq P_{nc,t}^{HL} \quad (20)$$

3.7. Generator

The power flow of each installed generator is modeled with a specific hourly variable $P_{G,d,nc,t}$ whose value is limited by the power output, its minimum working point and the generator status $z_{G,d,nc,t}$. All generators have the same per-unit fuel consumption within the operation range. The fuel consumption is the piece-wise linear function f with N_{FI} intervals, as detailed in (22). \tilde{g} is the interval corresponding to dispatching $P_{G,d,nc,t}$.

$$P_{G,d,nc,t}^{dg-} z_{d,nc,t}^G \leq P_{G,d,nc,t} \leq P_{G,d,nc,t}^{dg+} z_{d,nc,t}^G \quad (21)$$

$$F_{d,nc,t}^G = f_{\tilde{g},d,nc,t}^{int} P_{G,nc,t}^{dg} + f_{\tilde{g},d,nc,t}^{sl} P_{G,nc,t} z_{d,nc,t}^G \quad (22)$$

3.8. Tank

The fuel $V_{T,nc,t}$ stored in the tank must be lower than the total capacity considering degradation and aging, as modeled in (23). The formulation characterizes the amount of fuel stored in the previous time step $V_{T,nc,t}^{pre}$, the consumption of the generators $F_{d,nc,t}^G$ and the refilling variable $F_{nc,t}^{Fill}$, which is positive only when a refilling occurs and zero otherwise. When the tank is upgraded, the available fuel increases by a fixed ratio corresponding to the initial stored fuel.

$$0 \leq V_{T,nc,t} \leq \sum_{d \in pa(c)} V_{T,d,t}^{dg} \quad (23)$$

$$V_{T,nc,t} = V_{T,nc,t}^{pre} - \sum_{d \in pa(c)} F_{d,nc,t}^G + F_{nc,t}^{pre} \quad (24)$$

3.9. Degradation of components

The degraded capacity $X_{i,d,nc,t}^{dg}$ of each asset type i is modeled in (25) as a function of the remaining lifetime $RL_{i,d,nc,t}$ of each component, whose formulation is detailed in (26) as the difference between the remaining lifetime $RL_{i,d,nc,t}^{pre}$ of the same component in the previous time step and the wear $LL_{i,d,nc,t}$ occurred in the current time step. Variable $RL_{i,d,nc,t}^{pre}$, described in (27), equals the expected lifetime L_i of the component when it is either installed ($t = 1 \wedge d = n$) or replaced ($z_{i,d,nc,t}^R = 1$). Only the last installed component is replaced and this occurs when $z_{i,d,nc,t}^R$ equals one. In the other cases, the constraint sets the variable to the value of the previous time step: $RL_{i,d,nc,t-1}$ if it belongs to the

same branch or $RL_{i,d,p(n)n,end}$ otherwise. Finally, the lifetime loss $LL_{i,d,nc,t}$ of each component depends on the main aging determinant in (28), as described in Section 2.5.

$$X_{i,d,nc,t}^{dg} = X_{i,d,t} \frac{RL_{i,d,nc,t}}{L_i} \quad (25)$$

$$RL_{i,d,nc,t} = RL_{i,d,nc,t}^{pre} - LL_{i,d,nc,t} \quad (26)$$

$$RL_{i,d,nc,t}^{pre} = \begin{cases} L_i & t = 1 \wedge d = n \\ L_i & z_{R,i,d,nc,t} = 1 \\ RL_{i,d,p(n)n,end} & t = 1 \wedge d \neq n \\ RL_{i,d,nc,t-1} & \text{else} \end{cases} \quad (27)$$

$$LL_{i,d,nc,t} = \begin{cases} \delta^T & i \neq B \wedge \text{not aged} \\ \frac{P_{B,nc,t}}{E_{B,nc,t}^{dg}} & i = B \wedge \text{not aged} \wedge P_{B,nc,t} \geq 0 \\ 0 & \text{else} \end{cases} \quad (28)$$

3.10. Efficiency degradation

The efficiency degradation of the battery and converter is detailed in (29) as a function of the ratio between the remaining life of each component $RL_{i,d,nc,t}$ and the corresponding initial lifetime. The formulation accounts for the degradation status of components installed in different years. Multiple components of the same type are dispatched proportionally to their capacity and the equivalent efficiency $\eta_{i,nc,t}$ is calculated in (30), where η_i is the nominal efficiency of component type i , $\eta_{i,d,nc,t}^{act}$ is the actual efficiency for the component installed in node d and ϕ_i is the efficiency degradation rate. The degradation of generators is modeled in (31).

$$\eta_{i,d,nc,t}^{act} = \eta_i [1 - \phi_i (L_i - RL_{i,d,nc,t})], i \in \{B, D, I\} \quad (29)$$

$$\eta_{i,nc,t} = \frac{\sum_{d \in pa(c)} X_{i,d,nc,t}^{dg} \eta_{i,d,nc,t}^{act}}{\sum_{d \in pa(c)} X_{i,d,nc,t}^{dg}}, i \in \{B, D, I\} \quad (30)$$

$$f_{d,nc,t}^{sl/int} = f^{sl/int} [1 + \phi_G (L_G - RL_{d,G,nc,t})] \quad (31)$$

3.11. Fuel procurement

When the fuel available in the tank drops below a fixed threshold δ_T of the actual maximum capacity of the tank, a new fuel procurement is requested. The refill formulated in (32) occurs after a certain number of hours δt_{pdf} as delineated by a Monte Carlo process according to a specific probability density function pdf . The volume refilled is the fixed fraction v_T of the capacity of the tank.

$$F_{nc,t+\delta t_{pdf}}^{Fill} = v_T \sum_{d \in pa(c)} V_{T,d,t}^{dg} \quad (32)$$

4. Case study

The proposed method is tested for a microgrid in Wajir County in Kenya, whose main activities are in the agricultural sector. Due to the equatorial location, the proposed system is composed by photovoltaic plants, battery storage systems, converters, backup generators and the fuel tank. We assume a time horizon of 10 years, with a possible upgrade at the 5th year.

4.1. Load demand

The estimation of the load in a multi-year perspective faces two main challenges: estimating the shape of the daily load profile for every year and the energy growth. In this study, we propose a simplified approach where the shape changes homothetically along the years and the yearly energy growth rate is constant. Therefore, the hourly load profile of the y^{th} year is equal to a constant applied to the load profile. Moreover, in order to stress the stochastic analysis, a Gaussian hourly noise, with 20% standard deviation of the actual load, is introduced.

The load demand at the first year was estimated using data of a real system in the Wajir county, Kenya, for entire 2014 with 30-min intervals. Since the system has been operating for 8 years, the profile was discounted using the previous hypothesis to estimate the load profile of the microgrid in the first year. The yearly growth is tailored using monthly energy data for 23 microgrids in Kenya since their initial installation. By analyzing the 8 systems that been operated at least 8 years, we identified three linear growth rate scenarios at preset probabilities, according to Section 2: the so-called mid growth (27%), high growth (52%) and low growth (9%) scenarios with probabilities 60%, 20% and 20%, respectively. The full tree representation is depicted in Fig. 3: the lines represent the energy growth demand and the dots the upgrades. It is supposed that 20% of the actual load has high priority, being its curtailing more expensive (1 \$/kWh) than for the low priority demand (0.5 \$/kWh).

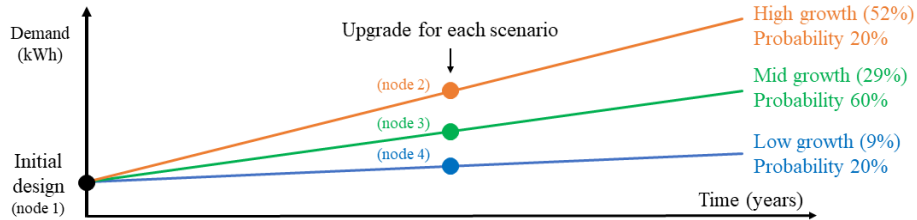


Figure 3: Tree structure of the case study, calibrated with data from 23 Kenyan microgrids: node 1 represents the initial design, nodes 3 to 5 correspond to the upgrades of the system for the high, mid and low growth rate scenario.

4.2. Renewable energy production

The photovoltaic energy production was estimated by using irradiance yearly profiles obtained with the Graham model [35, 36] and the combination of HDKR

and Herbs models [37], which together enable estimating the energy production by the irradiance and ambient temperature. The two-steps ARMA methodology of the Graham model captures the random deviations of the solar irradiance over a deterministic component related to the astronomical behavior specific for the site.

Since no data were available for the Wajir County, we calibrated the random characteristics of the Graham methodology with the data of the close weather station in Kitale, Kenya. The deterministic component and the average monthly irradiance of the Graham model, as well as the ambient temperature, were calibrated using data of the Wajir County.

4.3. Other parameters

The cost of components, as well as their maintenance, were assumed invariant with time. In particular, we assumed linear specific costs for batteries (350 \$/kWh) and the photovoltaic plant (800 \$/kWp). Moreover, the cost functions used for the fuel-fired generators, the converters, and the fuel tank are the same as in [1]. The maintenance costs for the photovoltaic plant, batteries, converters, and tanks are 16 \$/kWp/y, 3 \$/kWh/y, 2 \$/kW/y, and 0.15 \$/l/y, respectively. The minimum working point of the generator is 10% of its rated power, corresponding to a specific fuel consumption of 0.9 l/kWh. At its rated power, the value drops to 0.3 l/kWh. The maintenance cost of the generator is 5 c\$/kWp/h and the fuel price is 0.9 \$/l.

The lifetime of converters is assumed to be 15 years with high efficiency (96% for the inverter and 99% for the DCDC converter) that degrades by 0.13%/y. The efficiency of batteries (96% roundtrip) degrades by 5% at the end of its lifetime of 3000 equivalent cycles, corresponding to a capacity loss of 20%. The efficiency of the generator is assumed to decrease by 5% at the end of its lifetime (15000 operating hours). No degradation is assumed for the fuel tank, whose lifetime is 25 years.

The fuel procurement occurs when the fuel available in the tank reaches a fixed threshold (20%); then, the arrival of the refill occurs after a period of time drawn with a Weibull function, tailored so that at least 3 days are required to have a refill, which occurs within 6 days at 90% of probability.

4.4. Comparison procedure

The proposed multi-year stochastic approach (MYSA) is compared to a multi-year deterministic approach (MYDA), a MYDA with no upgrade (MYDA-NU) and standard 1-year methodologies (D5, D6, D7 and D10), as in [1]. The MYDA case study is developed using the same optimization approach as of MYSA but the load profile only corresponds to the mean scenario of Fig. 3. Moreover, we propose four 1-year case studies to evaluate whether the typical approach of designing the microgrid for the last year of the project could be improved. In particular, we performed a sensitivity analysis over the reference year to use in 1-year models and we propose case studies D5, D6, D7 and D10, whose load profile corresponds to the year 5th, 6th, 7th and 10th, respectively, of the mean load growth.

5. Results and discussion

The main results of the study are shown in Table 1 and Table 2, which details the NPC and the installed capacity for each component of the microgrid for every design methodology, respectively. Table 3 reports the NPC of the design achieved with 1-year models DXs and simulated under the multi-year behavior of MYSA. Finally, the fraction of energy-not-served of simulating the case D10 under MYSA conditions is depicted and compared in Fig. 4.

Table 1: Optimal solution, non-served energy and computational requirements with the multi-year stochastic approach (MYSA), the multi-year deterministic approach (MYDA) with mean load growth, the MYDA without upgrade (MYDA-NU), and the 1-year models (D5-D10).

Case	NPC [k\$]	Load Curt. [%]	Comp. time [h]
MYSA	953	2.3	69.9
MYDA	917	1.5	14.4
MYDA-NU	981	4.3	8.4
D10 (1-year)	1141	0.9	<0.2
D7 (1-year)	1034	1.1	<0.2
D6 (1-year)	935	1.1	<0.2
D5 (1-year)	825	0.9	<0.2

The outcomes reported in Table 1 confirm that the multi-year approaches achieve a cheaper solution than the typical 1-year methodology (D10), which optimizes the system for the demand of the 10th year. By considering the dynamics of the load growth, MYSA, MYDA and MYDA-NU enable a fine-tuned design of the system so that the initial design is smaller and the system is upgraded as demand grows and the components degrade. NPC of MYSA and MYDA is 16% and 20% lower than D10, respectively, thanks to the upgrade occurring 5 years after the first electrification; however, even when no upgrade is considered, such as in the MYDA-NU case, the NPC is still lower by 14% than that of D10, thus suggesting that multi-year approaches are worthy even without setting any upgrade.

As reported in Table 2, the installed capacity in the initial design (node 1) of multi-year approaches MYSA and MYDA is 40-50% lower than that of the D10 case, while the installed capacity at the 5th year of the mid scenario (node 3) almost equals the optimal design of D10, except for the tank and the generator. This means that some of the installed components are deferred in multi-year approaches, thus enabling savings in terms of NPC thanks to the discounting effect that discounts costs by 32% in 5 years. When no upgrade is considered (case MYDA-NU), NPC increases by 7% with respect to MYDA since no CAPEX are deferred and effects of components' degradation are stronger. Furthermore, the NPC in MYDA-NU is also lower than in D10, thanks to a significantly cheaper initial design, although the generators' consumption and the energy-not-served increase. All this suggests that 1-year models may capture the optimal long-term

Table 2: Installed capacity calculated with the approaches under test (MYSA, MYDA, MYDA-NU, and D5-D10); nodes numbering refers to Fig. 3.

Case	Node [#]	PV [kWp]	Batt. [kWh]	Inv. [kW]	DC/DC [kW]	Gener. [kW]	Tank [l]
MYSA	1	300	722	103	133	46	5782
	2	905	2414	296	428	158	12778
	3	577	1573	176	261	116	7416
	4	340	949	103	133	61	5782
MYDA	1	314	816	96	138	45	4262
	3	577	1571	168	271	116	7396
MYDA-NU	1	429	1011	158	179	74	8760
D10 (1-year)	1	588	1626	170	279	74	3003
D7 (1-year)	1	534	1470	253	154	62	2535
D6 (1-year)	1	473	1286	140	230	59	2834
D5 (1-year)	1	427	1184	121	200	51	1955

Table 3: Simulation of the 1-year design under multi-year behavior.

	D5	D6	D7	D10
Reference demand year [y]	5	6	7	10
NPC DX [k\$]	825	935	1034	1141
NPC DX-MYSA [k\$]	1119	1100	1119	1142
ENS DX-MYSA [%]	15.9	11.4	9.1	6.6

design of the system, but, by neglecting the load dynamics, they incur in higher costs and sub-optimal financial plans, contrarily to multi-year approaches.

The savings in CAPEX achieved by multi-year approaches are slightly counteracted by higher load curtailment and fuel costs with respect to 1-year models, as highlighted in Table 1. However, according to Fig. 4, load curtailment costs occur only years after the last installation, which means that it is economically cheaper not to tailor each upgrade to supply the demand of the last year, given the proposed cost parameters, the proposed discount rate and scenario tree. The load curtailment peaks at about 24% only in the 5th year of the high growth scenario because the initial design is sized considering a weighted average of all scenarios, whereas the high-scenario has only 20% of probability to occur. In the mid scenario of MYSA and MYDA, it is never higher than 7% and lower than 2% in the last year, thanks to the upgrade. In MYDA-NU, where no upgrade is considered, load curtailment increases up to about 12% in the last year of the project, although the first installation was higher than in MYDA. This suggests that upgrading the microgrid as demand grows not only decreases NPC but also increases the service quality by reducing ENS, and the proposed approach can help the developer tailor the upgrading plan for its specific project according to

its requirements.

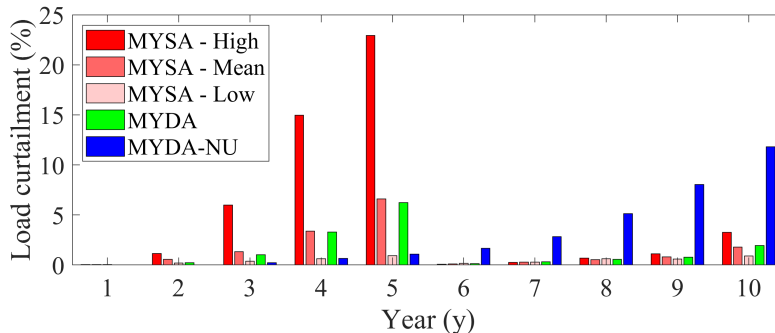


Figure 4: Fraction of the energy-not-served of multi-year case studies.

Despite providing interesting results, multi-year approaches have high computational requirements (8-70h), thus they can be more suitable for the advanced design of the microgrid rather than preliminary studies, which might be better served by 1-year models. High computational costs (70 h) of MYSA are justified by a fine evaluation of the NPC under uncertainties in the load growth conversely to MYDA and 1-year models. MYDA approximates well the optimal design of the mid scenario of MYSA with lower computational requirements (14 h), but neglect uncertainties. As a consequence, NPC of MYDA is slightly lower than MYSA by 4%. MYDA-NU requires only 8 h, but has higher NPC and ENS, since it has no upgrade and neglects uncertainties.

Although the proposed case study has strong symmetries related to the growth rates (52%, 39% and 9%), scenarios' probabilities (20%, 60% and 20%) and the invariant shape hypothesis, the installed capacities at the 5th year are not completely linear with the growth rate, also due to the economies of scale. For instance, the inverter, the DC/DC converter and the tank are not upgraded in the low growth scenario, due to economies of scale, the discount rate, and reduced energy-not-served. Although out of the scope of this paper, MYSA can easily handle stronger asymmetries in growth scenarios, which can affect the results and especially the initial design which is common for all scenarios.

It is worth noticing that since the yearly load profiles of 1-year models (DXs) differ from the one of multi-year cases, be them stochastic (MYSA) or deterministic (MYDA), the optimal NPC of cases DXs cannot be a measure of the NPC subject to the multi-year behavior of the demand. Aiming at evaluating such difference, we reported in Table 3 the NPC (NPC DX-MYSA) and the ENS of the microgrid designed with the 1-year methodology (cases D5-D10) and simulated with the same multi-year approach of MYSA depicted in Fig. 3. The sensitivity analysis over the reference mid-term demand highlights that the gap between NPC DX and NPC DX-MYSA increases from D10 to D5 due to a sharp increase in fuel consumption and load curtailment, whose ratio reaches up to 15% in D5-MYSA. This suggests that underestimating the load demand has

high consequences in terms of NPC and ENS. Furthermore, it is worth noticing that even the lowest ENS (6.6%) with D10-MYSA is much higher than the corresponding one in Table 1, as D10 simulations neglect the stochastic behavior of the demand growth and its dynamics. Considering also that no NPC with DX-MYSA is comparable to NPC with MYSA, MYDA or MYDA-NU, results suggest that it is difficult for 1-year models to be as cheap as multi-year ones, thus the latter can fine-tune the business plan.

6. Conclusions

The present study addressed the optimal planning and dynamic capacity expansion of rural microgrids in developing countries, considering the degradation of components and uncertainties in the forecast of the load profile and its growth rate. Particle Swarm Optimization has been successfully used in multi-year planning, comprising for hourly simulations of the multi-year lifetime of the system. Uncertainties of the load growth have been considered by means of a scenario-tree formulation. The operational consequences of the assets' degradation are also simulated.

The case study based on data collected from Kenyan microgrids confirmed that the NPC of the proposed multi-year approach was 16-20% lower than in standard 1-year methodologies, where only the last year of the project is simulated and operational effects of components' degradation are neglected. Contrary to standard approaches, the capacity expansion proposed here enables deferring the components' installation as demand grows, thus strongly reducing CAPEX and NPC. Fuel consumption and energy-not-served slightly increase over time to compensate for the demand growth and the components' degradation, but their negative effects on NPC are limited, also due to the discount effect.

A sensitivity analysis over the load forecast of 1-year methodologies suggested that no single 1-year load forecast can approximate the solution achieved by a multi-year method. The same results highlighted that underestimating the demand in 1-year models leads to high costs and large share of energy-not-served, when no upgrade takes place.

Results show that 1-year methodologies successfully calculate the optimal long-term design of the system with very low computational requirements; however, the solution of multi-year approaches is more fine-tuned, since they evaluate the multi-year behavior of the system, including load growth and components' degradation. Therefore, 1-year methods could be suitable for a preliminary design, while multi-year approaches are more advisable in later planning stages.

This study can lay the foundation for further stochastic multi-year approaches based on heuristic methodologies even considering multiple energy sources, non-linear behavior of components or reliability concerns, which are timely topics with space for improvement.

References

- [1] D. Fioriti, R. Giglioli, D. Poli, G. Lutzemberger, A. Micangeli, R. Del Citto, I. Perez-Arriaga, P. Duenas-Martinez, Stochastic sizing of isolated rural mini-grids, including effects of fuel procurement and operational strategies, *Electr Pow Syst Res* 160 (2018) 419–428.
- [2] E. Hartvigsson, E. O. Ahlgren, Comparison of load profiles in a mini-grid: Assessment of performance metrics using measured and interview-based data, *Energy Sustain. Dev.* 43 (2018) 186–195.
- [3] A. Micangeli, R. Del Citto, I. Kiva, S. Santori, V. Gambino, J. Kiplagat, D. Viganò, D. Fioriti, D. Poli, Energy Production Analysis and Optimization of Mini-Grid in Remote Areas: The Case Study of Habaswein, Kenya, *Energies* 10 (12) (2017) 2041.
- [4] S. Mandelli, J. Barbieri, R. Mereu, E. Colombo, Off-grid systems for rural electrification in developing countries: Definitions, classification and a comprehensive literature review, *Renewable and Sustainable Energy Reviews* 58 (2016) 1621–1646.
- [5] Y. Liu, S. Yu, Y. Zhu, D. Wang, J. Liu, Modeling, planning, application and management of energy systems for isolated areas: A review, *Renewable and Sustainable Energy Reviews* 82 (October 2017) (2018) 460–470.
- [6] P. V. Gomes, J. T. Saraiva, A two-stage strategy for security-constrained AC dynamic transmission expansion planning, *Electric Power Systems Research* 180 (2020) 106167.
- [7] G. Gutiérrez-Alcaraz, N. González-Cabrera, E. Gil, An efficient method for Contingency-Constrained Transmission Expansion Planning, *Electric Power Systems Research* 182 (2020) 106208.
- [8] P. Duenas, A. Ramos, K. Tapia-Ahumada, L. Olmos, M. Rivier, J. I. Pérez-Arriaga, Security of supply in a carbon-free electric power system: The case of Iceland, *Applied Energy* 212 (November 2017) (2018) 443–454.
- [9] A. Ehsan, Q. Yang, Optimal integration and planning of renewable distributed generation in the power distribution networks: A review of analytical techniques, *Applied Energy* 210 (2018) 44–59.
- [10] F. Riva, F. Gardumi, A. Tognollo, E. Colombo, Soft-linking energy demand and optimisation models for local long-term electricity planning: An application to rural India, *Energy* 166 (2019) 32–46.
- [11] H. Fathtabar, T. Barforoushi, M. Shahabi, Dynamic long-term expansion planning of generation resources and electric transmission network in multi-carrier energy systems, *Int. J. of Electr. Power and Energy Syst.* 102 (February) (2018) 97–109.

- [12] H. Ranjbar, S. H. Hosseini, Stochastic multi-stage model for co-planning of transmission system and merchant distributed energy resources, *IET Generation, Transmission and Distribution* 13 (14) (2019) 3003–3010.
- [13] M. Ahmadigorji, N. Amjady, S. Dehghan, A novel two-stage evolutionary optimization method for multiyear expansion planning of distribution systems in presence of distributed generation, *Applied Soft Computing Journal* 52 (2017) 1098–1115.
- [14] M. C. da Rocha, J. T. Saraiva, A multiyear dynamic transmission expansion planning model using a discrete based EPSO approach, *Electric Power Systems Research* 93 (2012) 83–92.
- [15] M. H. Shaban Boloukat, A. Akbari Foroud, Stochastic-based resource expansion planning for a grid-connected microgrid using interval linear programming, *Energy* 113 (2016) 776–787.
- [16] A. Khodaei, S. Bahramirad, M. Shahidehpour, Microgrid Planning Under Uncertainty, *IEEE Trans. Pow. Syst.* 30 (5) (2015) 2417–2425.
- [17] Y. Liu, R. Sioshansi, A. J. Conejo, Multistage Stochastic Investment Planning With Multiscale Representation of Uncertainties and Decisions, *IEEE Transactions on Power Systems* 33 (1) (2018) 781–791.
- [18] H. Mehrjerdi, Dynamic and multi-stage capacity expansion planning in microgrid integrated with electric vehicle charging station, *Journal of Energy Storage* 29 (2020) 101351.
- [19] Z. K. Pecenak, M. Stadler, K. Fahy, Efficient multi-year economic energy planning in microgrids, *Applied Energy* 255 (2019) 113771.
- [20] H. Alharbi, K. Bhattacharya, Stochastic Optimal Planning of Battery Energy Storage Systems for Isolated Microgrids, *IEEE Transactions on Sustainable Energy* 9 (1) (2017) 1–1.
- [21] N. Nguyen-hong, H. Nguyen-Duc, Y. Nakanish, Optimal sizing of energy storage devices in wind- diesel systems considering load growth uncertainty, *IEEE Trans. Ind. Appl.* 54 (3) (2018) 54–59.
- [22] E. Hajipour, M. Bozorg, M. Fotuhi-Firuzabad, Stochastic Capacity Expansion Planning of Remote Microgrids with Wind Farms and Energy Storage, *IEEE Trans. Sustain. Energy* 6 (2) (2015) 491–498.
- [23] Z. Wang, Y. Chen, S. Mei, S. Huang, Y. Xu, Optimal expansion planning of isolated microgrid with renewable energy resources and controllable loads, *IET Renew Power Gener* 11 (7) (2017) 931–940.
- [24] Y. Zhang, J. Wang, A. Berizzi, X. Cao, Life cycle planning of battery energy storage system in off-grid wind-solar-diesel microgrid, *IET Generation, Transmission and Distribution* 12 (20) (2018) 4451–4461.

- [25] R. C. Guerrero, M. A. A. Pedrasa, An MILP-Based Model for Hybrid Renewable Energy System Planning Considering Equipment Degradation and Battery Lifetime, 2019 IEEE 2nd International Conference on Power and Energy Applications, ICPEA 2019 (2019) 207–211.
- [26] N. Sharma, Varun, Siddhartha, Stochastic techniques used for optimization in solar systems: A review, Renewable and Sustainable Energy Reviews 16 (3) (2012) 1399–1411.
- [27] D. Fioriti, D. Poli, P. Cherubini, G. Lutzemberger, A. Micangeli, P. Duenas-Martinez, Comparison among deterministic methods to design rural mini-grids: Effect of operating strategies, IEEE PowerTech 2019 (2019) 1–6.
- [28] M. Ecker, N. Nieto, S. Käbitz, J. Schmalstieg, H. Blanke, A. Warnecke, D. U. Sauer, Calendar and cycle life study of Li(NiMnCo)O₂-based 18650 lithium-ion batteries, Journal of Power Sources 248 (2014) 839–851.
- [29] A. Sangwongwanich, Y. Yang, D. Sera, F. Blaabjerg, Lifetime Evaluation of Grid-Connected PV Inverters Considering Panel Degradation Rates and Installation Sites, IEEE Trans. Power Electron. 33 (2) (2018) 1125–1236.
- [30] Homer Energy, HOMER Pro 3.13 User Manual, Tech. rep. (2019).
- [31] S. Barsali, M. Ceraolo, R. Giglioli, D. Poli, Storage applications for Smart-grids, Electric Power Systems Research 120 (2015) 109–117.
- [32] W. Römisch, Scenario Reduction Techniques in Stochastic Programming, Springer, Berlin, Heidelberg, 2009, pp. 1–14.
- [33] C. D. Barley, C. B. Winn, Optimal dispatch strategy in remote hybrid power systems, Solar Energy 58 (4-6) (1996) 165–179.
- [34] M. Sedghi, A. Ahmadian, M. Aliakbar-Golkar, Optimal storage planning in active distribution network considering uncertainty of wind power distributed generation, IEEE Trans. Pow. Syst. 31 (1) (2016) 304–316.
- [35] V. A. Graham, K. G. T. Hollands, T. E. Unny, A Time Series Model for Kt with Application to Global Synthetic Weather Generation, Solar Energy 40 (2) (1988) 83–92.
- [36] V. A. Graham, K. G. T. Hollands, A method to generate synthetic hourly solar radiation globally, Solar Energy 44 (6) (1990) 333–341.
- [37] J. A. Duffie, W. A. Beckman, Solar Engineering of Thermal Processes, 4th Edition, John Wiley and Sons, Inc., Hoboken, NJ, USA, 2013.